ARTIGO ORIGINAL
DOI: 10.5433/1679-0375.2017v38n2p43

Crateras e Pits de Cavitação em Metais

Cavitation Erosion Pits and Craters in Metals

Gil Bazanini[1]

Resumo

Foram obtidos erosão e "pits" de cavitação utilizando o dispositivo a disco rotativo, onde um disco contendo indutores de cavitação e os corpos de prova giram em uma câmara preenchida com água, visando causar escoamento cavitante. Estes "pits" puderam ser observados com auxílio de um microscópio eletrônico de varredura. Micro-jatos oriundos do colapso da bolha, ou cavidade, geralmente causam danos à superfície sólida próxima . Os danos causados pelo colapso apresentam formato próximo do esférico. Pelo fato de serem causados por micro-jatos, os "pits" e demais danos apresentam formato esférico. Finalmente, foi calculado o "pit counting" que consiste no número de "pits" por unidade de área e de tempo. Observou-se ainda a influência da velocidade de escoamento no "pit counting" : quanto maior a velocidade, maior o valor do "pit counting" calculado.Também foram estudadas as "crateras" resultante do contato da bolha com o corpo de prova, em como a influência de altas temperaturas (3.000 K) no fenômeno, resultando ainda em manchas escuras em volta das crateras.
Palavras-chave: Cavitação. "Pits". Erosão. Crateras. Metais.

Abstract

Cavitation pits and erosion were obtained using the rotating disk device, where a steel disk with cavitation inducers and specimens fixed on it rotates inside a water chamber to provide the cavitating flow. These pits were observed with the aid of a scanning electronic microscopy. Micro-jets impingement resulting from bubble (or cavity) collapse cause damages to solid surfaces on the proximity. Because they are caused by the micro-jets, these pits are spherical. Finally, the pit counting, that is, the number of pits by area and by time unit was calculated. The influence of the flow velocity was also studied here, and how greater is the flow velocity, how greater is the pit counting calculated. It is also studied here other remaining effects (such as "craters") left during the bubble collapse, High values of temperature (3,000 K) calculated can explain the craters from bubble impactions and the dark spots around them.
Keywords: Cavitation. Pits Erosion Craters Metals.

[1] Departamento de Engenharia Mecânica da Universidade do Estado de Santa Catarina, gil.bazanini@udesc.br

Introduction

Damage by cavitation is a complex phenomenon that includes hydrodynamic, mechanic, metallurgical and chemical processes (BERCHICHE; FRANC; MICHEL, 2000). Here, the phenomenon was observed for aluminum and 1020 carbon steel specimens. The cavitation phenomenon, that is, the formation, growth and collapse of air and vapor bubbles in liquids is, as well known, responsible for damage in metallic and non-metallic solid structures in liquid mediums, remarkably in water. Such bubbles, also named cavities, nucleate from micro-bubbles of air present in the liquid medium. Such bubble formation phenomenon is named "cavitation inception" (HAMMITT, 1980). The growth process involves primarily the action of pressure forces, and these are the results of the interplay of surface action, inertia, viscosity (BAZANINI; HOAYS, 2008). In most simple terms, it is the balance of the static force at the bubble wall between the surface tension and pressure differences caused by physical properties.

As it growths, the bubble is filled by the liquid vapor, present when the pressure and temperature of the mixture are close to the vapor pressure and temperature of the surrounding liquid, until reaching an maximum equilibrium radius (YOUNG ,1989). The most usual example is the cavitation erosion in centrifugal pumps (HATTORI; KISHIMOTO, 2008). Liquid micro-jets impingement, through bubbles close to the solid surface, lead to surface damages such as plastic deformation and materials loss from the wall. These micro-jets are caused by bubble final stages of collapse near the solid surface (and influenced by its presence); a good visualization of the phenomenon can be seen in Shervani-Tabar, Rezaee-Barmi and Mahmoudi (2003) and others for the final stages of collapse. Thus, the micro-jets and bubble final impaction against the solid surface is the responsible for loss of material from the surface or plastic deformation.

To a better understanding of the phenomena, the effects of cavitation on solid surfaces, several devices have been developed along the last decades, such as the cavitation test chamber (STELLER et al., 2005). The jet-impact damage device (JANAKIRAM, 1973) consists of water liquid jets impinging in specimens fixed on rotating disks, the reduce the time of the experiments, there is the vibratory apparatus (KNAPP et al., 1970) where the specimens are set to vibrate in the test liquid, the vertical (related to the axis) rotating disk (CHENG; JIANG; LIANG, 2013) where a disk with the specimens fixed on it is rotating in water to provide cavitating flow, and finally (the most important, because it reproduces quite well the phenomenon of the flow through a centrifugal pump) the horizontal rotating disk device (VIVEKANANDA, 1983; ZHIYE, 1983).

Experimental Apparatus

Specimens fixed on the disk surface and close to the cavitation inducers (holes in the present tests) are kept in a cavitating flow inside the chamber. To prevent vibration problems, the holes and the specimens are situated on opposite radial positions of their reciprocals. Vibration absorbers are also used at the equipment foundations, and the disk mounted with the tests specimens is balanced before tests were performed. Details of the apparatus can be seen in Figure 1.

Figure 1 – Side view of the test rig and the frequency inverter

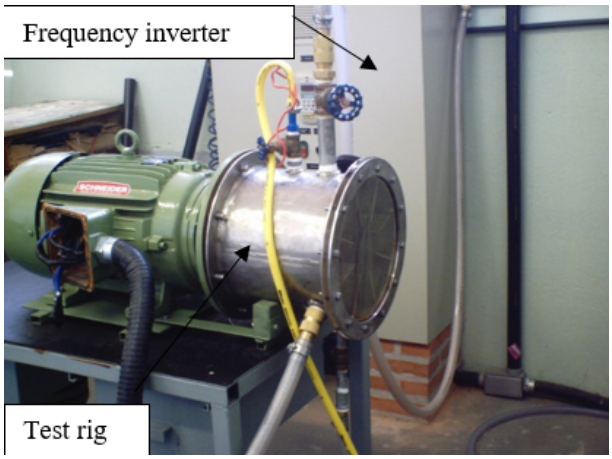

Source: The Author.

For cooling purposes, a water reservoir is used to circulate the water in the chamber, being the piping provided by control valves and a filter to protect the pump from small particles resulting from the erosion.

The results obtained for the chemical elements of the materials tested here are shown in Table 1.

Local high temperature impaction of the bubble and micro-jets against the specimens in the final stages of the collapsing cavities, results in pits and craters.

The disk and the chamber are made by stainless steel, more resistant to cavitation erosion. It was made a compact version of the device, that is, smaller chamber and disk diameter (250 mm), as well as a shorter shaft. By using the "Intermediary Device", commonly used to connect pumps to electric motors, we can avoid the use of the bearing and the coupling, resulting in a shorter shaft. That is, the chamber now replaces the pump. This reduces loss transmissions as well as alignment problems. The Intermediary Device is made by bronze, also to prevent corrosion.

Table 1 – Chemical composition of the specimens

Chemical element (%)	Carbon Steel	Aluminium
C	0,21	-
Pb	-	0,01
Zn	-	0,02
Al	0,01	98,24
Fe	98,60	0,22
Si	0,23	0,45
Cu	0,04	0,16
Mn	0,68	0,22
Mg	-	0,68

Source: The Author.

Connections for inlet and outlet of water, temperature and pressure visualizations, and water drain and air outlet are also provided. Eight baffles equally spaced were welded in the chamber (and at a distance 18 mm from the disk) to kept bubbles to collapse over the test specimens and to minimize rotation of the test fluid and generate the desired cavitation effects.

A frequency inverter is used to control the motor operation, and thus the disk rotation, that was kept at 4400 rpm.

Some authors in a recent past have being using a carburized cast iron chamber and protruding pins mounted on the disk. Here, the disk and the chamber are made by stainless steel, more resistant to cavitation erosion.

Method

Experimental Procedure

Inlet and outlet valves are used to control temperature and pressure inside the chamber that is connected to an overhead water reservoir. Temperature and pressure in the chamber are also monitored by a thermometer and a manometer of scales 0-100 ^{o}C and 0-3 bar, respectively. The speed of the electric motor (and then the water flow velocity on the specimens) is controlled by a frequency inverter that may also be used to obtain the power consumption.

After each 5 hours operating in cavitating conditions, the specimens are cleaned by ultrasound and dried. Images of the specimens were also obtained using a scanning electronic microscope (SEM).

In present work, aluminum and 1020 carbon steel were used as test specimens. To fix the disk to the to electric motor shaft, a flange was specially manufactured in bronze.

Temperature Calculations

Recently, specimen surface analysis of cavitation erosion by bubble collapse provided a temperature higher then 300 ^{o}C, when working with a vibratory device, even reaching 6,000 ^{o}C, according to Chen, Li and Liu, (2009).

For the bubble temperature calculations, it is taking into account the initial gas pressure P_{g0}, the initial vapor pressure P_{v0}, the adiabatic constants of the gas and vapor, K_g and K_v , and the liquid and gas viscosities μ_L and μ_g, respectively.

For the gas and the vapor trapped inside the bubble, it will also be considered the effect of the van der Waals hard core a_g and a_v (Barber et al., 1997). So, gas and vapor are being considered to obey the van der Waals equation of state for real gases. This is important because of the raising pressures inside the bubble during the collapse.

$$T = \frac{T_0}{(P_{v0}+P_{g0})}\left[\frac{P_{g0}R_0^{3(k_g-1)}}{\left(R^3-a_g^3\right)^{(k_g-1)}}+\frac{P_{v0}R_0^{3(k_v-1)}}{(R^3-a_v^3)^{(k_v-1)}}\right]. \quad (1)$$

Using Equation (1), the temperature as a function of the radius was calculated (BAZANINI, 2003), reaching a maximum value of about 3,000 K for the bubble contents, in its final stages of collapse for a bubble of an average size (radius of 1mm, for example). Anyway, there are always such high temperature values in that compression. P_∞ is the pressure in a position far enough in the liquid (where no effects of the collapse are felt), and R_0 the cavity initial radius. T_0 is the cavity (or bubble) internal initial temperature.

It is known for a long time that heat conduction in fluids may occur when they are in direct contact at different temperatures (LANDAU; LIFSHITZ, 1959). In this case, certainly there is some heat conduction from the bubble to the surrounding liquid. That fact should minimize the bubble temperature increase when compared to the adiabatic case, that is, assuming the bubble collapse too fast for conduction heat transfer to occur. It is one of the objectives here to verify such adiabatic hypothesis, by estimating the temperature variation in the bubble due to the heat transfer, as well as the conduction heat transfer.

Making the energy balance for the bubble, we should have

$$3k\frac{dT}{dR}4\pi R^2 = PdV + \frac{dE}{dt}, \quad (2)$$

Where k is the conduction heat transfer coefficient (0.7 for the water in the international system of units), E is the bubble energy, and V the volume. That will result an Equation to estimate the temperature reduced ("cooling effect") in the bubble contents temperature as the collapse proceeds:

$$\Delta T = \frac{\frac{P_\infty R_0^3}{3}\left(\frac{1}{R_0} - \frac{1}{R}\right) + \frac{P_\infty}{6}\left(R_0^2 - R^2\right)}{3k}. \quad (3)$$

The high temperature in the bubble leads to the formation of a thermal boundary layer in the liquid during the bubble collapse. This boundary layer is usually assumed to be linear, and can be calculated by Equation (4) (Frank and Michel, 2005):

$$\delta_T = \sqrt{\frac{k}{\rho_L C_P t}}, \quad (4)$$

where δ_T is the boundary layer thickness, ρ_L is the liquid density, C_P is the specific heat of the water, and t is the time of the collapse.

Results

The so called "Pit Counting", that is, the number of pits per square millimeters per hour, was calculated to compare with existing ones, although the literature is very limited in providing information for this kind of damage comparison. Anyway, a comparison is made in Table 2, just in the intent of quality purposes.

Table 2 – Results for the "pit counting", comparing with the existing in the references (for qualitative purposes only, because of the differences in the experiments).

	Material	Flow velocity (m/s)	pits/(mm^2x hour)
Saito/Sato	Al	3,6	0,71
Present work	Al	41,8	1,33
Present work	Carbon steel	36,8	1,00

Source: The Author.

It was also observed some dark spots around the cavitation pits and crates, as can be seen in the Figures 2 to 6.

The temperature increases by the compression of the mixture vapor-air. Since the collapse phenomenon is too fast (about some micro-seconds, or even less), the question

Figure 2 – Aluminum, after 5 hours of tests, magnification of 50x

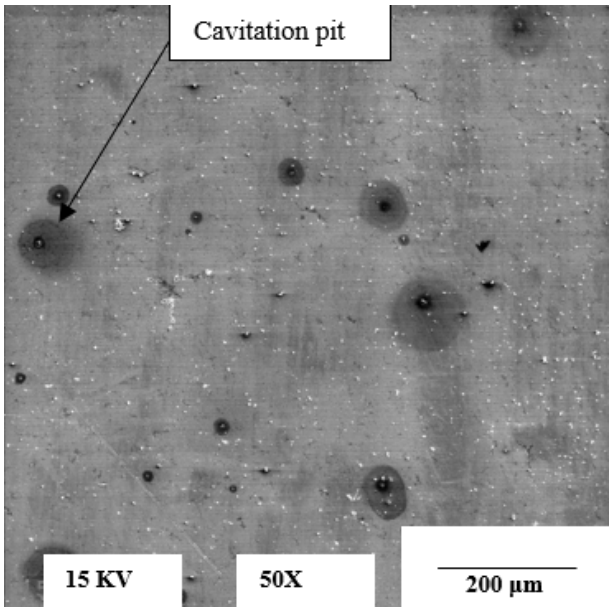

Source: The Author.

Figure 3 – Aluminum, magnification of 200x, after 10 hours of tests.

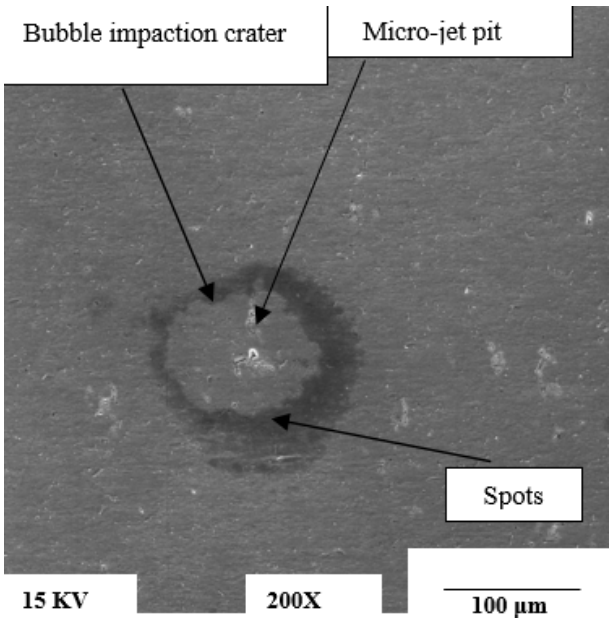

Source: The Author.

Figure 4 – Aluminum test specimen after 15 hours of tests in cavitating conditions with magnification of 200x.

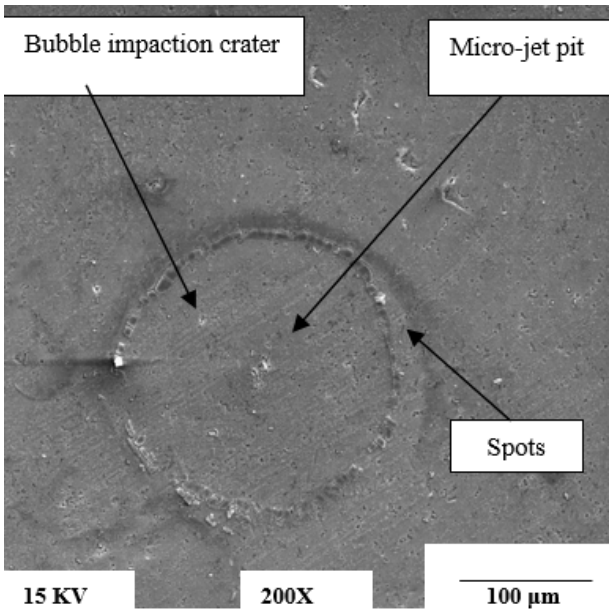

Source: The Author.

is if there is enough time for conduction heat transfer from the bubble to the liquid to reduce substantially the increase of the bubble internal temperature, as the collapse proceeds.

Figure 5 – carbon steel after 5 hours of tests, magnification of 50x.

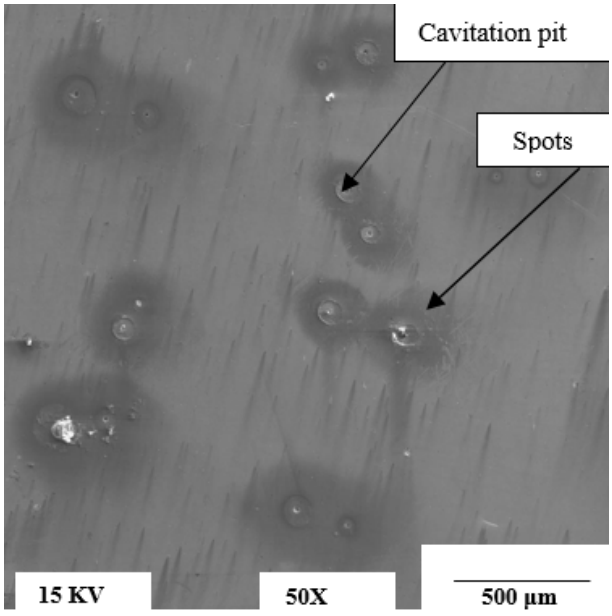

Source: The Author.

As the bubble collapses there is an internal reduction is its contents temperature due to heat conduction to the surrounding liquid. That reduction in the temperature was calculated using Equation (3), and the results are shown in Table 3, where the temperature reduction (a cooling effect) was calculated for two normal bubble radii. It agrees with

Figure 6 – Spots around cavitation pits,. carbon steel, magnification of 200x, after 5 hours of tests.

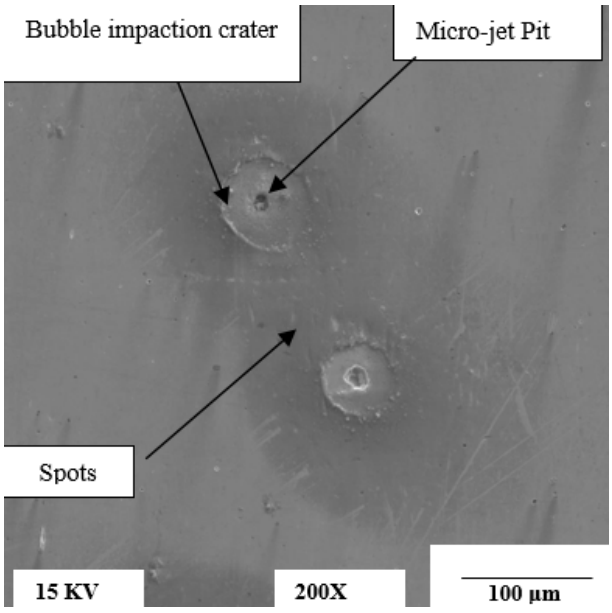

Source: The Author.

the fact that how greater is the radius, greater is the heat transfer area.

Table 3 – Temperature reduced by convection heat transfer during bubble collapse, calculated by Equation (3).

Bubble initial radius R_0 (mm)	3.56	1.0
Temperature reduction (K) due to heat conduction to the liquid	15	0.9

Source: The Author.

Using Equation (4), it was also calculated the thermal boundary layer along the surrounding liquid, caused by the bubble contents heating because of the compression process, in the final stage of the collapse, with a radius of about 0.4 mm, as shown in Figure 7. The variables used in Equation (4) are, in the international system of units: ρ_L 998, C_P 4,180. For the time of collapse it was considered a value 0.7 ms (BAZANINI, 2003b).

Discussion

The cavities collapsing near the specimen surfaces, led to some cavitation damage as usual, basically by micro-jets impingement formed during the collapse, and hot bubble impaction against the solid surface in the end of

Figure 7 – Thermal Boundary Layer in the Final Stage of the Bubble Collapse.

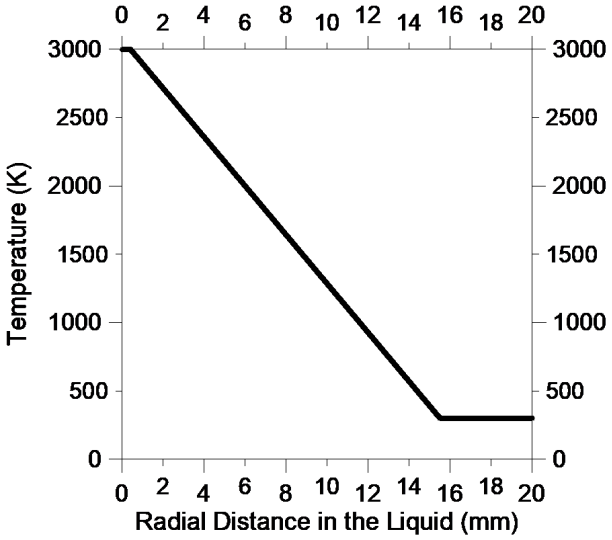

Source: The Author.

the phenomenon, plus pressure waves in the case of bubble having more then one collapse.

Cavitation pits and craters were observed on the images after some time in test conditions for the aluminum and the carbon steel specimens, as well as dark spots around them.

For the aluminum specimen (Figure 2), the results of the cavitation "Pit Counting" presented in Table are only for qualitative purposes since the time considered for each test conditions were different from each other and we must remember that damage by cavitation is exponential time performed. Saito and Sato (2003) realized their tests by 2 hours, while in the present work the performing time of testes for the pit counting in cavitating conditions in (Figure 2) was 5 hours.

Besides, the velocity attained for Saito and Sato (2003) was de 3.6 m/s. In the device used in these experiments attained velocities from 36.8 m/s to 41.8 m/s.

For the carbon steel (Figure 5) the "pit counting" resulted in about 1 pit/(mm2 x hour), when working of a flow velocity of 36,8 m/s, but it was no found other researches results for a good comparison with these data. We expect this data could motivate researchers to performer experiments working these data (or similar ones), for comparison purposes.

These "pits" obtained her were about 100 μm in diameter close to the final bubble dimensions.

The cooling effect for the bubble contents resulted negligible, since it was observed a reduction of 15 K for a bubble internal temperature of 3,000 K, approximately.

When bubble radius is 0.4 mm, already in the final stage of the collapse, the radial distance of the thermal boundary layer extends to about 15 mm.

Conclusions

Pits and Crater areas were seen in the cavitation pits regions. The micro-jet pits are usually in the center of the damage region because of their creation process in the bubble, that is, through the collapsing bubble.

Anyway, all specimens showed some kind of damage after the tests.

Although the pit counting measured here and compared with existing results on the references, it showed some agreeable results, this method was not efficient for erosion measurement, neither for comparison results. Besides, if the specimen used is of some material that has a good erosion tax, it becomes difficult to count and make comparisons. The pits are removed by erosion as the tests proceed, among other parameters and the materials do not have the same erosion tax. Perhaps mass or volume (or area as well) loss becomes a more efficient method of comparison.

The spots and craters observed are very likely formed by heat released from plastic surface deformation caused by high temperature impaction of the bubble contents on the final stage of the collapse process. The values of temperature calculated can explain reasonably well the craters from bubble impactions and the spots on the temperature on the thermal boundary layer, where the temperature goes from 3,000 K close to bubble to 300 K.

So, these bubble impaction crater areas and dark spots found in aluminum and carbon steel test specimens become the bubble "final act", with the aid of eventually pressure waves formed by possible bubble oscillations in this already chaotic scenario.

Finally, the cooling effect due to bubble conduction to the surrounding liquid resulted negligible, keeping high temperature values inside the bubble until the end of the collapse and marking the metallic test specimens.

References

BARBER, B. P.; HILLER, R. A.; LÖFSTEDT, R.; PUTTERMAN, S. J.; WENINGER, K. R. *Defining the unknowns of sonoluminescence*. Physics Reports, v. 281, n. 2, p. 65-143, March 1997.

BAZANINI, G. *Temperature calculation inside collapsing bubbles in compressible liquids*. 2nd. Brazilian Congress on Manufacturing Engineering, Uberlandia, Brazil, 2003a.

BAZANINI, G. *Compressible bubble dynamics in viscous compressible liquids with pressure field calculation*. 2^{nd}. Brazilian Congress of ManufacturingEngineering, Uberlandia, Brazil, 2003b.

BAZANINI, G.; HOAYS, S. H. *Oscilações de cavidades na forma adimensionalizada*. In: ENCONTRO BRASILEIRO SOBRE EBULIÇÃO, CONDENSAÇÃO E ESCOAMENTO MULTIFÁSICO LÍQUIDO- GÁS, 1., 2008, Florianópolis. Anais... Florianópolis, abril, 2008. p.1-5.

BERCHICHE, N.; FRANC, J. P.; MICHEL, J. M. *Un Modèle de prédiction de lérosion dês matériaux ductiles par la cavitation. mécanique dês fluides*. Academie des Scienses., Paris,France, Éditions Scientifique et Médicales. Elsevier. 2000.

CHEN, H. S., LI, J., LIU, S. H.. *A ring area formed around the erosion pit on 1Cr18Ni9Ti stainless steel surface in incipient cavitation erosion*. Wear, n. 266, p. 884-887, 2009.

CHENG, F. JIANG S., LIANG J *Cavitation erosion resistance of microarc oxidation coating on aluminium alloy*. Applied Surface Science, n. 280, p. 287-296, 2013.

FRANK, J. C.; MICHELL, J. P. *Fundamentals of Cavitation*. Paris,France, Kluwer Academic Publishers, 2005.

HATTORI, S.; KISHIMOTO, M. *Prediction of cavitation erosion on stainless steel in centrifugal pumps*. Wear, 265, 1870-1874, Nov, 2008.

HAMMITT, F. G. *Cavitation and multiphase flow phenomena*. New York, USA,McGraw-Hill Book Company, 1980.

JANAKIRAM, K. S. *Studies on erosion due to liquid jet impingement*. MSc. Thesis, Indian Institute of Science, Bangalore, June, 1973.

KNAPP, R. P.; DAILY, J. W.; HAMMITT, F. G. *Cavitation*. New York,USA,McGraw- Hill 1970.

LANDAU, L. D.; LIFSHITZ, E. M. *Course of theoretical physics*. London, England, Pergamon Press, 1966. v.. 6. Fluid Mechanics. Ship Scientific Research Center Report, China, 1983.

SAITO, S., SATO, K. *Cavitation bubble collapse and impact in the wake of a circular cylinder*. In: Fifth International Symposium on Cavitation, Osakaa, Japan, November, 2003.

SHERVANI-TABAR, M. T.; REZAEE- BARMI, A.; MAHMOUDI, S. M. S. *Velocity field and pressure distribution around two parts of a cavitation bubble after its splitting near a rigid boundary*. In: Fifth International Symposium on Cavitation, Osaka, Japan, 2003.

STELLER, J.; KRELLA, A.; KORONOWICZ, J.; JANICKII, W. *Towards quantitative assessment of material resistance to cavitation, erosion*. Wear, 258, p. 604-613, 2005.

VIVEKANANDA, P. *Mechanism of cavitation damage influence of stacking fault energy on erosion and erosion resistance of steels and coatings*. Ph.D. Thesis, Dept. Of Civil Engineering, Indian Institute of Science, Bangalore, India, 1983.

YOUNG, F. R. *Cavitation*. London, England, McGraw-Hill Book Company, 1989.

ZHIYE, J. *An experimental investigation on cavitation erosion for propeller alloys*. China Ship Scientific Research Center Report, China, 1983.

Nomenclature

a_g van der Waals hard core for the gas
a_v van der Waals hard core for the vapor
C_P specific heat
E energy
K conduction heat transfer coefficient
K_g adiabatic constant of the gas
K_v adiabatic constant of the vapor
P_{g0} initial gas pressure
P_{v0} initial vapor pressure
P_∞ pressure far away in the liquid
R bubble radius
R_0 bubble initial radius
t time
T temperature
T_0 bubble internal initial temperature
V volume
δT thermal boundary layer thickness
μ_g gas viscosity
μ_L liquid viscosity
ρ_L liquid density

Recebido em 9 Setembro, 2016– Received on September 9, 2016
Aceito em 22 Outubro, 2017– Accepted on October 22, 2017